Thermal Stress Analysis in Ultra-Thin Whitetopping Pavement

J.R. Roesler & D. Wang
University of Illinois at Urbana-Champaign, Urbana, Illinois USA

ABSTRACT: Minimizing joint opening is crucial to ensure adequate load transfer across the joints in ultra-thin whitetopping (UTW) pavement. Several UTW parking lot projects completed at the University of Illinois indicated that the initial joint cracks occurred at every 5 to 8 joints (for 4 by 4 ft panels). The result of this large crack spacing was wider openings at these initial crack locations and reduced load transfer. The primary objective of this theoretical thermal stress calculation for UTW was to determine if the initial crack spacing at early ages (e.g., 24 hours) can be approximately predicted for UTW sections, and if it is possible to promote additional cracks to propagate at early ages. The two types of thermal stresses considered are axial thermal stress due to uniform temperature change in the slab and curling stress due to temperature differential through the slab thickness. Temperature profile data and laboratory elastic and fracture parameters are presented for several concrete mixtures at early ages. The analytical model coupled with the measured data revealed that 4 by 4 ft UTW panels will not crack at every saw-cut joint for the concrete mixtures and climatic conditions evaluated. Larger joint spacing, such as 6 by 6 ft, is sufficient but still may not propagate cracks at every joint. Initiating more joint cracks at early ages can be attained by higher stresses in the concrete layer (e.g., more slab restraint or longer slab sizes), lower material fracture properties, or a deeper notch depth.

1 INTRODUCTION

Several challenges in ensuring an ultra-thin whitetopping (UTW) pavement meets the service life objective are preserving bond between the concrete and existing asphalt concrete layer, and maintaining adequate load transfer across the joints. Since no man-made load transfer devices exist across the contraction joints, the crack width or joint opening must be minimized to maintain aggregate interlock. Several ways to minimize joint opening include smaller slab sizes and selecting concrete mixtures with low heat of hydration, low drying shrinkage potential, or with the inclusion of fiber-reinforcement. Selection of a small slab size will only promote good load transfer if uniformly distributed working cracks exist at early ages. Several UTW projects completed at the University of Illinois in the summer of 2006 and 2007 (Roesler et. al 2008) indicated that many of the contraction joints did not crack initially. In fact, the initial joint cracks occurred at every 5 to 8 joints (for 4 x 4 ft panels). The result of this large crack spacing was wider openings at these initial crack locations and reduced load transfer. Cracks at other locations eventually propagated, but the load transfer efficiency (LTE) across these cracks were dramatically higher than the initial cracks.

The primary objective of this analytical study was to determine if the initial crack spacing at early ages (e.g., 24 hours) can be approximately predicted for UTW sections, and if it is possible to promote additional cracks to propagate at early ages. One additional factor, which has made it more difficult to propagate cracks at early ages, is the addition of fibers, which increase the crack propagation resistance of the concrete. The nonlinear mechanical behavior of the fiber reinforcement was difficult to account for in conjunction with the selected nonlinear elastic fracture mechanics model presented in this study.

There are two types of thermal stresses generated, namely axial thermal stress due to uniform temperature change in the slab, and curling stress, due to temperature differential through the

slab thickness. For simplicity, only linear temperature differentials throughout the slab are considered. Field and laboratory data are presented for several concrete mixture designs at early ages. Finally, a discussion is presented to interpret the field observations and results of the analytical model.

2 SOLUTION METHODS FOR AXIAL THERMAL STRESS

To calculate the axial thermal stress due to uniform temperature change in the slab, two mechanistic-based methods are used. The first one was developed using one-dimensional elasticity theory with a bilinear slab-base friction assumption (Zhang and Li, 2001). This one-dimensional model was modified to predict the time-dependent joint opening in jointed plain concrete pavement (JPCP) due to climatic loadings (Roesler and Wang, 2008). The solution method generates a spatially dependent axial thermal stress. The one-dimensional model takes slab geometries into consideration, such as slab thickness h and length L; in addition the model includes a few other material properties, such as the elastic modulus of the concrete E, the steady-state slab-base frictional stress τ_0, and its corresponding slab slippage δ_0, where τ_0 and δ_0 can be determined from a field test. This solution method is abbreviated as the "Bilinear Model" in this paper. Although UTW assumes the concrete is bonded to the underlying asphalt layer, there is field evidence that local debonding occurs under certain conditions and therefore at early ages a slab-base friction assumption is deemed valid. A second method was introduced by Westergaard in 1926 and is based on a two-dimensional elasticity theory. Only the maximum axial thermal stress in the interior area of a large slab can be calculated. As expected, the derived formula is independent of slab geometric conditions. To facilitate the introduction of the Bilinear Model, the underlying bilinear slab-base interfacial restraint model is presented first (Roesler and Wang, 2008).

2.1 *Slab-subbase interfacial restraint*

Let x be the direction along the Portland cement concrete (PCC) slab length, z be the direction along the PCC slab thickness, where z is measured positive downward and $z = 0$ is at the mid-depth of slab. The ends of the slab are located at $x = 0$ and $x = L$. It is assumed that no displacement occurs at the mid-span of the slab $x = L/2$, thus only half of the slab ($0 \le x \le L/2$) is analyzed. The coordinate system is shown in Figure 1.

The slab-base friction interaction serves as a restraint to slab movement, thus proper characterization of this friction is critical for accurately predicting the axial thermal stress in the concrete slab. Field push-off test results suggest that the stress-slippage behavior of a slab-base interface can be satisfactorily approximated by a bilinear function as presented in equation (1) below (Rasmussen and Rozycki, 2001; Wimsatt et al. 1987):

$$\tau(x) = \begin{cases} \dfrac{\tau_0}{\delta_0} u(x) & \text{if } |u(x)| \le \delta_0 \\ \tau_0 & \text{if } 0 < \delta_0 < u(x) \\ -\tau_0 & \text{if } u(x) < -\delta_0 < 0 \end{cases} \tag{1}$$

where $\tau(x)$ is the slab-base interfacial friction at x (MPa), and a stress sign convention is applied (Timoshenko and Goodier, 1970); τ_0 is the steady-state friction (MPa); δ_0 is the slippage (displacement) corresponding to the friction of τ_0 (mm); $u(x)$ is the average displacement through the PCC slab thickness (mm). In cases where $u(x) > 0$, the PCC slab contracts, and where $u(x) < 0$, the PCC slab expands for $0 \le x \le L/2$. Equation (1) is plotted in Figure 2.

2.2 *Maximum thermal Stress, σ_m based on bi-linear model*

Equation (1) and Figure 2 suggest that there are two cases for which axial thermal stress development should be studied. The maximum axial thermal stress σ_m for each case is listed below and the derivation can be found in Roesler and Wang (2008).

Figure1. Coordinate system used in this model

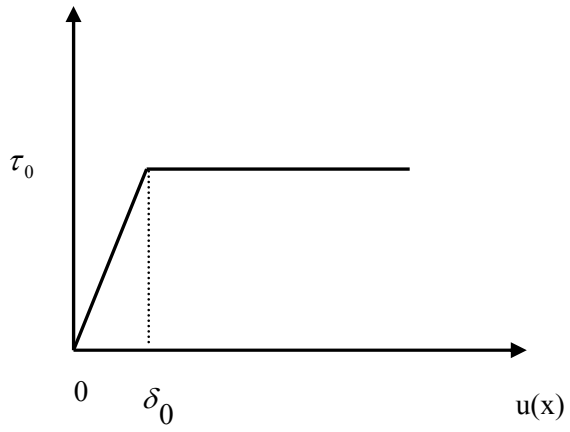

Figure 2. Bilinear Slab-subbase restraint mode

- Case 1 occurs when $u(0) \le \delta_0$, thus

$$\sigma_m = -E\alpha \cdot \Delta T_{ave}\left[1 - \frac{1}{\cosh(\beta L/2)}\right] \tag{2}$$

- Case 2 occurs when $u(0) \ge \delta_0$ and $u(x_0) = \delta_0$, thus

$$\sigma_m = -E\alpha \cdot \Delta T_{ave}\left[1 - \frac{1}{\cosh(\beta(0.5L - x_0))}\right] + E\beta^2\delta_0 x_0 \frac{1}{\cosh(\beta(0.5L - x_0))} \tag{3}$$

Here, E and μ are the modulus of elasticity and Poisson's ratio of concrete, respectively; ΔT_{ave} is the temperature difference between uniform (or average) temperature at time t in the slab and slab setting temperature, where the method for calculating average temperature in the slab is presented in Section 3; α is the coefficient of thermal expansion of concrete; h is the slab thickness ; $\beta = \sqrt{\frac{\tau_0}{Eh\delta_0}}$; x_0 is the coordinate value of x where the displacement u equals δ_0 (x_0 can be numerically determined using equation 4 via a nonlinear equation solver, such as Newton-Raphson iterative method described by Burden and Faires, 2001).

$$\delta_0 = -\frac{1}{\beta}\left[\beta^2\delta_0 x_0 + \alpha \cdot \Delta T_{ave}\right]\frac{e^{-\beta x_0} - e^{-\beta(L-x_0)}}{e^{-\beta x_0} + e^{-\beta(L-x_0)}} \tag{4}$$

2.3 *Westergaard's axial thermal stress formula*

Westergaard's formula for calculating the maximum thermal stress, assuming an infinite slab length, is given in equation 5 (Westergaard 1926) as

$$\sigma_m = \frac{E\alpha \cdot \Delta T_{ave}}{1-\mu} \tag{5}$$

As mentioned above, the Westergaard solution is the maximum axial thermal stress induced in the central part of a large slab, where horizontal displacements due to uniform temperature changes are assumed to be fully resisted by the slab-base frictional restraint. Equation (5) always over-estimates the axial thermal stress value since finite slab sizes exist in reality. The Westergaard axial thermal stress serves as the upper bound for axial thermal stresses calculated using other mechanistic models and therefore, should be interpreted with caution.

3 CURLING STRESS DUE TO LINEAR TEMPERATURE DIFFERENTIAL THROUGH SLAB THICKNESS

Westergaard's curling stress formula for the case of a slab having infinite width and finite length L can be applied (Westergaard 1926). The maximum tensile or compressive stress σ at the top of the slab in the middle of slab length is (derived from Westergaard 1926)

$$\sigma = \sigma_0 \left[1 - \frac{2(\sin\lambda\cosh\lambda + \cos\lambda\sinh\lambda)}{\sin 2\lambda + \sinh 2\lambda} \right] \tag{6}$$

where $\sigma_0 = \frac{E\alpha \cdot \Delta T_c}{2(1-\mu)}$; $\lambda = \frac{L}{l\sqrt{8}}$; $l = \sqrt[4]{\frac{Eh^3}{12(1-\mu^2)k}}$; and ΔT_c is the temperature difference between the top and the bottom of slab, under the assumption of a linear temperature difference through the thickness; and k is the modulus of subgrade reaction.

The linear temperature difference between the top and the bottom of slab $\Delta T_c(t)$, can be extracted from a measured nonlinear temperature profile using the concept of an equivalent linear temperature component (Ioannides and Khazanovich, 1998). Given the measured temperature profile through the thickness of slab, $T(z,t)$, the average temperature through the thickness of slab, $T_{ave}(t)$, which is needed in the axial thermal stress calculation can be approximated in equation (7) using the mean-value theorem of integration in calculus.

$$T_{ave}(t) = \frac{1}{h}\int_{-h/2}^{h/2} T(z,t)dz \tag{7}$$

Also, $\Delta T_c(t)$ is given in equation (8) (Roesler and Wang 2008)

$$\Delta T_c(t) = T_L(-\frac{h}{2},t) - T_L(\frac{h}{2},t) = -\frac{12}{h^2}\int_{-h/2}^{h/2} \xi T(\xi,t)d\xi \tag{8}$$

where T_L is the equivalent linear temperature component.

4 THERMAL STRESS CALCULATIONS

The main inputs for the calculation of thermal stresses based on the above methods are listed as: temperature profile, setting temperature, elastic modulus, base parameters, and the soil k-value.

4.1 *Temperature profile*

The temperature profile through the thickness of slab is critical in the thermal stress development at early ages, also the temperature profile in the slab during the first 24 hours plays an important role in selecting the appropriate saw-cutting for UTW (including saw-cut timing, joint spacing, etc), slab temperature data measured at different depths for times t = 6, 8, 10, 12, and 24 hours after the slab was cast was used and listed in Table, where the slab thickness is 4.5 inch. Furthermore, the average temperature and equivalent linear temperature differential calculated using equations (7) and (8), respectively are listed in Table 2.

Table 1: Measured Concrete Slab Temperature at Different Depths (°C)

Time After Slab Cast (hrs)	Surface	1 in.	2 in.	4.5 in.
6	47.73	48.39	48.41	45.06
8	44.68	45.18	45.56	44.56
10	39.41	40.97	42.10	42.72
12	35.50	36.99	38.22	39.69
24	31.32	31.33	31.36	31.44

Table 2: Calculated Average Temperature and Linear Temperature Differential (°C)

Time After Slab Cast (hrs)	Mean temperature	ΔT ($T_{top} - T_{bottom}$)
6	47.03	4.87
8	44.99	0.72
10	41.79	-3.62
12	38.22	-5.07
24	31.38	-0.18

4.2 *Setting Temperature*

The setting temperature is assumed to be 50°C, and inferred to occur at t = 5 hours after the slab was cast, based on the observation of temperature profile measured at 15-minute intervals.

4.3 *Elastic modulus of concrete*

The elastic modulus of concrete E is an important material parameter used in any elasticity theory-based thermal stress formulation. Since no early concrete material data was available for this particular UTW project, elastic moduli of six different concrete mixtures tested in the laboratory were used. The elastic modulus values are given in Table 3. Note the concrete mixture nomenclature in Table 3 (e.g., 555.44) stands for the 555 lb/yd^3 of cementitious materials, 0.44 water to cement ratio, and 'st' means a 25mm maximum aggregate size was used instead of 38mm.

Table 3. Elastic Modulus of Concrete at Early Ages (MPa)

Mixture	6 hours	8 hours	10 hours	12 hours	24 hours
Mix 3 (Anna, IL)	7,331	9,468	11,452	13,283	21,049
Mix 11 (Dan Ryan)	3,360	4,480	5,601	6,721	13, 441
555.44	1,635	4,542	7,766	11,820	16,843
555.44st	1,196	3,322	5,679	8, 643	12,316
688.38	1,180	3,277	5,603	8, 528	12,152
688.38st	1,368	3,800	6,496	9, 888	14,090

4.4 *Base parameters*

The parameters used in the bilinear slab-base restraint model for concrete placed on an asphalt layer are: τ_0 = 0.052 MPa and δ_0 = 0.38 mm.

4.5 *K-value*

The k-value or modulus of subgrade reaction used in Westergaard's curling stress formula is assumed to be 100 psi/in.

4.6 *Maximum Axial Thermal Stress*

The maximum axial thermal stress are given in Table 4 for different joint spacing calculated using the Bilinear Model for Mix_3 (Anna, IL), along with those based on Westergaard's formula, which is independent of joint spacing. Table 4 demonstrates that the maximum axial thermal stress only varies slightly with large joint spacing from 120 ft to 240 ft. Thus, only the maximum axial thermal stress based on the Bilinear Model for L taken between 12 ft and 120 ft were considered for the rest of mixture analyses in this study. Thermal stresses for joint spacing less than 12 ft were not calculated since the tensile stresses were very small.

Table 4. Maximum Axial Thermal Stress Based on Bilinear Model for Mix 3 (Anna) *(MPa)*

Joint Spacing *L* (ft)	Time Elapsed (hrs)				
	6	8	10	12	24
12	0.0501	0.0882	0.148	0.217	0.357
20	0.104	0.193	0.335	0.502	0.837
24	0.128	0.242	0.428	0.648	1.073
28	0.148	0.286	0.512	0.785	1.304
30	0.156	0.305	0.551	0.848	1.417
40	0.187	0.380	0.707	1.113	1.956
60	0.214	0.453	0.872	1.412	2.849
80	0.222	0.478	0.935	1.537	3.431
100	0.225	0.487	0.959	1.587	3.748
120	0.225	0.490	0.968	1.607	3.907
140	0.225	0.491	0.971	1.615	3.984
160	0.226	0.491	0.972	1.618	4.021
180	0.226	0.491	0.973	1.619	4.040
200	0.226	0.491	0.973	1.620	4.048
220	0.226	0.491	0.973	1.620	4.053
240	0.226	0.491	0.973	1.620	4.055
Westergaard's Result	0.265	0.578	1.145	1.906	4.772

In the first 24 hours after the whitetopping pavement is cast, the fully restrained (or bonded) condition between PCC slab and existing asphalt concrete (AC) layer may not be well develop. In this paper, equation (1) was adopted to describe the shear stress acted on PCC slab by AC layer. This slab-base friction assumption generates reasonable maximum axial thermal stress for Mix 3 (Anna). Furthermore, the full restraint assumption based on Westergaard's formula serves as an upper bound of the maximum axial thermal stresses as seen in Table 4.

Table 5 lists the curling stresses at the top of the slab for different joint spacing values for Mix_3. As expected, Table 5 shows that Westergaard's curling stress values remain unchanged in the first three or four decimal places when L was greater than 40 ft ($L/l \rightarrow \infty$). Therefore, only the curling stresses for L ranging from 12 ft to 40 ft for the other mixtures were considered.

Table 5. Curling stress for Mix 3 (Anna) (MPa)

Joint Spacing *L* (ft)	Time Elapsed (hrs)				
	6	8	10	12	24
12	-0.236	-0.0449	0.268	0.429	0.0222
20	-0.219	-0.0425	0.259	0.424	0.0249
24	-0.216	-0.0417	0.253	0.412	0.0231
28	-0.217	-0.0416	0.251	0.408	0.0226
30	-0.217	-0.0417	0.251	0.408	0.0225
40 to 240	-0.217	-0.0418	0.252	0.410	0.0226

5 ANALYSIS OF SAW-CUTTING PATTERN

The material fracture properties, K_{IC} and c_f, are required for calculation of the nominal strength of the concrete slab at early ages. Table 6 presents the experimental fracture properties for the six concrete mixtures at 6, 8, and 10 hours. Table 7 lists the nominal strength of concrete slab (σ_N) for the Mix_3 (Anna) mixture versus the notch depth-to-slab thickness ratio (*a/d*), where *a* is the notch depth and *d* is the slab thickness. σ_N is calculated using Bazant's size effect model and measured concrete fracture properties (K_{IC} and c_f) at several ages. The detailed explanation of this model is contained in the paper by Gaedicke et al. (2007).

Table 6. Critical stress intensity factors (K_{IC}) and c_f values at early age.

AGE	Mixture					
	Mix 11	Mix 3	555.44	555.44st	688.38	688.38st
Hours	K_{IC} (MPa-$m^{0.5}$)					
6	0.01	0.16	0.03	0.02	0.05	0.03
8	0.02	0.22*	0.12	0.07	0.17	0.10
10	0.04	0.33	0.19	0.19	0.33	0.26
Hours	c_f (m)					
6	0.027	0.062	0.069	0.027	0.0014	0.0014
8	0.001	0.040*	0.037	0.031	0.0030	0.0018
10	0.004	0.016	0.026	0.018	0.0048	0.012

*estimated values

Table 7. Nominal Strength (σ_N) for Mix 3 (MPa)

Time	Notch Depth-to-Slab Thickness Ratio									
(hrs)	0.0	0.1	0.2	0.3	0.4	0.5	0.6	0.7	0.8	0.9
6	0.268	0.301	0.284	0.267	0.243	0.212	0.178	0.145	0.116	0.092
8	0.493	0.490	0.450	0.415	0.375	0.327	0.276	0.226	0.182	0.144
10	1.279	1.026	0.874	0.771	0.682	0.595	0.507	0.422	0.344	0.275

Given the nominal strength of concrete slab (σ_N) and the combined maximum tensile thermal stress σ for a fixed joint spacing at a particular time (Tables 4 plus 5 stresses), the minimum saw-cut depth to slab thickness ratio (*a/d*) can be determined by setting σ equal to σ_N from Table 7 for Mix_3 (Anna). A set of notch depth ratios required for equilibrating the nominal strength of the concrete to the maximum tensile stress for various joint spacing at different saw-cutting times are given in Table 8 for Mix_3 (Anna).

Table 8. Saw-Cut Depth to Slab Thickness Ratio (a/d) for Slab Made by Mix 3 for Different Joint-Spacing

Joint spacing *L* (ft)	Concrete Ages					
	6 hrs		8 hrs		10 hrs	
	Tensile Stress	*a/d*	Tensile Stress	*a/d*	Tensile Stress	*a/d*
12	0.28 (Bottom)		0.043	Too early	0.416	0.7
20	0.323 (Bottom)		0.151	Too early	0.594	0.5
24	0.344 (Bottom)		0.200	0.75	0.681	0.4
28	0.365 (Bottom)		0.244	0.65	0.763	0.3
30	0.373 (Bottom)		0.263	0.6	0.802	0.25
40	0.404 (Bottom)		0.338	0.5	0.959	0.15
60	0.431 (Bottom)		0.411	0.30	1.124	0.05

The tensile stresses presented in Table 8 are the superposition of the axial thermal stress and maximum tensile curling stress; the tensile stress is calculated at the top of slab, except at $t = 6$ hours where it is greatest at the bottom of the slab due to daytime curling stresses. In the case of maximum tensile stresses at the bottom of the slab, no saw-cut depth suggestion is made since cracks will initiate at the bottom and propagate upward if tensile stresses are above the nominal strength of the concrete slab. However, these bottom tensile stresses assume that the material does not creep. The tensile creep at early ages has been reported to relax stresses as much as 50

percent (Grasley 2006), which would reduce these bottom stresses below the material strength. The nominal strengths of concrete slab (σ_N) made by the other mixtures at different notch depth-to-slab thickness ratios (*a/d*) are given in Tables 9, 11, 13, 15, and 17, and the corresponding saw-cut notch depth ratio (*a/d*) based on critical tensile stress (thermal) are given in Tables 10, 12, 14, 16, and 18, respectively.

Table 9. Nominal Strength (σ_N) for Mix 11 (Dan Ryan) (MPa)

Time (hrs)	Notch Depth-to-Slab Thickness Ratio									
	0.0	0.1	0.2	0.3	0.4	0.5	0.6	0.7	0.8	0.9
6	0.035	0.032	0.029	0.026	0.023	0.020	0.017	0.014	0.011	0.009
8	0.272	0.092	0.067	0.055	0.048	0.042	0.036	0.030	0.025	0.021
10	1.279	0.156	0.119	0.100	0.087	0.075	0.065	0.055	0.045	0.037

Table 10. Saw-cut Depth to Slab Thickness Ratio (a/d) for Mix 11 (Dan Ryan) for Different Joint Spacing

Joint spacing *L* (ft)	Concrete Ages					
	6 hrs		8 hrs		10 hrs	
	Tensile Stress	*a/d*	Tensile Stress	*a/d*	Tensile Stress	*a/d*
12	0.148 (Bottom)		0.0541	0.3	0.265	0.05
20	0.170 (Bottom)		0.120	0.08	0.380	Too late
24	0.180 (Bottom)		0.144	0.07	0.429	Too late
28	0.187 (Bottom)		0.162	0.06	0.469	Too late
30	0.190 (Bottom)		0.169	0.06	0.486	Too late
40	0.198 (Bottom)		0.193	0.04	0.542	Too late
60	0.203 (Bottom)		0.208	0.04	0.585	Too late

Table 11. Nominal Strength (σ_N) for Mix 555.44 (MPa)

Time (hrs)	Notch Depth-to-Slab Thickness Ratio									
	0.0	0.1	0.2	0.3	0.4	0.5	0.6	0.7	0.8	0.9
6	0.058	0.053	0.051	0.048	0.044	0.038	0.032	0.026	0.021	0.016
8	0.314	0.275	0.252	0.231	0.209	0.182	0.154	0.126	0.102	0.081
10	0.594	0.498	0.443	0.401	0.358	0.313	0.265	0.219	0.177	0.141

Table 12. Saw-cut Depth to Slab Thickness Ratio (a/d) for Mix 555.44 for Different Joint Spacing

Joint spacing *L* (ft)	Concrete Ages					
	6 hrs		8 hrs		10 hrs	
	Tensile Stress	*a/d*	Tensile Stress	*a/d*	Tensile Stress	*a/d*
12	0.0801 (Bottom)		0.0541	0.3	0.265	0.05
20	0.0913 (Bottom)		0.121	0.70	0.467	0.15
24	0.0944 (Bottom)		0.145	0.60	0.534	0.05
28	0.0962 (Bottom)		0.164	0.55	0.592	0.0
30	0.0968 (Bottom)		0.171	0.50	0.618	Too late
40	0.0983 (Bottom)		0.195	0.45	0.711	Too late
60	0.0988 (Bottom)		0.211	0.40	0.794	Too late

Table 13. Nominal Strength (σ_N) for Mix 555.44st (MPa)

Time (hrs)	Notch Depth-to-Slab Thickness Ratio									
	0.0	0.1	0.2	0.3	0.4	0.5	0.6	0.7	0.8	0.9
6	0.096	0.069	0.057	0.049	0.043	0.038	0.032	0.027	0.022	0.018
8	0.200	0.172	0.155	0.141	0.127	0.111	0.085	0.077	0.062	0.050
10	0.713	0.565	0.487	0.432	0.384	0.335	0.260	0.237	0.192	0.154

Table 14. Saw-cut Depth to Slab Thickness Ratio (a/d) for Mix 555.44st for Different Joint Spacing

Joint spacing *L* (ft)	Concrete Ages					
	6 hrs		8 hrs		10 hrs	
	Tensile Stress	*a/d*	Tensile Stress	*a/d*	Tensile Stress	*a/d*
12	0.0614 (Bottom)		0.0532	0.85	0.267	0.65
20	0.0687 (Bottom)		0.1034	0.55	0.383	0.40
24	0.0703 (Bottom)		0.1194	0.45	0.434	0.30
28	0.0712 (Bottom)		0.1314	0.35	0.474	0.25
30	0.0714 (Bottom)		0.1354	0.30	0.491	0.20
40	0.072 (Bottom)		0.1484	0.25	0.549	0.10
60	0.0722(Bottom)		0.1564	0.20	0.593	0.05

Table 15. Nominal Strength (σ_N) for Mix 688.38 (MPa)

Time (hrs)	Notch Depth-to-Slab Thickness Ratio									
	0.0	0.1	0.2	0.3	0.4	0.5	0.6	0.7	0.8	0.9
6	0.797	0.236	0.171	0.141	0.122	0.106	0.092	0.078	0.065	0.053
8	1.564	0.739	0.557	0.466	0.404	0.352	0.303	0.256	0.212	0.172
10	2.351	1.337	1.039	0.878	0.764	0.666	0.573	0.482	0.398	0.322

Table 16. Saw-cut Depth to Slab Thickness Ratio (a/d) for Mix 688.38 for Different Joint Spacing

Joint spacing *L* (ft)	Concrete Ages					
	6 hrs		8 hrs		10 hrs	
	Tensile Stress	*a/d*	Tensile Stress	*a/d*	Tensile Stress	*a/d*
12	0.0607 (Bottom)		0.053	Too early	0.265	1.00
20	0.0678 (Bottom)		0.1026	Too early	0.380	0.80
24	0.0695 (Bottom)		0.1186	Too early	0.429	0.75
28	0.0703 (Bottom)		0.1295	Too early	0.469	0.70
30	0.0706 (Bottom)		0.1345	Too early	0.486	0.70
40	0.0712 (Bottom)		0.1465	0.95	0.542	0.60
60	0.0713(Bottom)		0.1545	0.95	0.585	0.55

Table 17. Nominal Strength (σ_N) for Mix 688.38st (MPa)

Time (hrs)	Notch Depth-to-Slab Thickness Ratio									
	0.0	0.1	0.2	0.3	0.4	0.5	0.6	0.7	0.8	0.9
6	0.478	0.142	0.103	0.085	0.073	0.064	0.055	0.047	0.039	0.032
8	1.126	0.453	0.335	0.278	0.240	0.210	0.181	0.153	0.127	0.103
10	1.196	0.871	0.725	0.632	0.557	0.485	0.415	0.346	0.283	0.227

Table 18. Saw-cut Depth to Slab Thickness Ratio (a/d) for Mix 688.38st for Different Joint Spacing

Joint spacing *L* (ft)	Concrete Ages					
	6 hrs		8 hrs		10 hrs	
	Tensile Stress	*a/d*	Tensile Stress	*a/d*	Tensile Stress	*a/d*
12	0.0689 (Bottom)		0.0539	Too early	0.290	0.80
20	0.0777 (Bottom)		0.1113	0.9	0.418	0.60
24	0.0798 (Bottom)		0.1303	0.8	0.475	0.50
28	0.0810 (Bottom)		0.1442	0.75	0.523	0.45
30	0.0814 (Bottom)		0.1502	0.70	0.543	0.40
40	0.0823 (Bottom)		0.1672	0.65	0.615	0.30
60	0.0826 (Bottom)		0.1782	0.60	0.673	0.25

6 DISCUSSION

The maximum axial thermal stress calculations using the Bilinear Model in Table 4 suggest that increases in stress are linked with increases in joint spacing and the maximum axial stress ap-

proaches the theoretical maximum axial stress calculated based on Westergaard's formula (from Equation (5)) for very large slab sizes. The Westergaard solution for maximum axial stress does not accurately assess the crack spacing development in concrete pavements, especially in the first 24 hours.

Equations (2), (3), (5) and (6) used for computing thermal stresses are influenced by the elastic moduli of the concrete. It is clear that Mix_3 (Anna), representing a high early strength concrete, exhibits the highest elastic moduli at early ages among the six mixtures studied here. As expected, Mix_3 (Anna) attains the largest axial thermal stress among the six mixtures with all other conditions the same.

In the concrete mixtures presented in Tables 8, 12, 14, 16, and 18 (excludes Mix_11), the concrete strength gain is high enough that the induced thermal stresses will not be able to propagate the cracks at the pre-determined notch depth ratio of 0.25 to 0.33 and panel size of 4 ft. In fact, cracks will not initiate at 12 ft spacing for this thermal history and concrete material parameters. Cracks will only propagate at longer spacing (20 to 40 ft) due to the effect the slab length has on the axial stress development as the concrete material cools the first night. This is very consistent with the UTW field observation that typically results in every 5^{th} to 8^{th} saw-cut joint propagating a crack, i.e., 20 to 32 ft spacing between propagated joint cracks. Table 10 is the one exception to the aforementioned behavior. This concrete mixture contained 35 percent slag and gains strength and elastic modulus more slowly. As shown in Table 10, it is much easier to propagate cracks at early ages, i.e., the required notch depth ratios are very small (< 0.25).

There may be a means to increase the elastic modulus of the concrete without proportionally increasing its strength gain. However, this may be very difficult without significant research to develop appropriate strategies and material combinations. Furthermore, the main factors in the concrete modulus of elasticity are related to the aggregate type and aggregate volume. One active way of potentially propagating the cracks is thermally cooling the surface of the slab (using water and wind) after the peak concrete temperatures have been reached. This has some appeal since it would limit early-age drying shrinkage, however, it may promote de-bonding of the concrete from the underlying asphalt concrete layer before the bond strength has developed sufficiently. Another promising technique to assure early age joint cracks at the desired spacing may be to dynamically fracture the joint with a mechanical device (Cockerell 2007).

7 SUMMARY

From this Ultra-Thin Whitetopping (UTW) study, the field observation, laboratory testing, and analytical analysis support each other in terms of the observed cracking pattern at the joints after the first 24 hours. Certainly, selecting of "best" saw-cutting pattern for an UTW project is a complicated task, since it involves accurate early age prediction of pavement temperature profile, thermal stress fields, and characterization of the specific concrete material mechanical properties. This study reveals that 4 by 4 ft UTW panels will not crack at every saw-cut joint for the given climatic condition and concrete mixture types analyzed and tested. The analytical study suggests that initial larger joint spacing, such as 6 by 6 ft, is fine but still may not propagate cracks at every joint. Shorter slab sizes such as 4 x 4 ft are not necessarily detrimental especially in parking lots since they reduce the shear stress at the concrete-asphalt interface and these slab sizes reduce later age curling and loading stresses.

ACKNOWLEDGMENTS

This publication is based on the results of ICT-R27-3A *Design and Concrete Material Requirements for Ultra-Thin Whitetopping*. ICT-R27-3A was conducted in cooperation with the Illinois Center for Transportation; the Illinois Department of Transportation, Division of Highways; and the U.S. Department of Transportation, Federal Highway Administration. A special thanks to Matt Beyer for his collection of the temperature profile data and early-age elastic and fracture parameters.

8 REFERENCES

Burden, R.L. & Faires, J.D. (Seventh Edition) 2001. *Numerical Analysis*. Brooks/Cole.

Cockerell, A. 2007. Method and Apparatus for Forming Cracks in Concrete, U.S. Patent No. 7,308,892.

Gaedicke, C., Villalobos, S., Roesler, J. & Lange, D. 2007. Fracture mechanics analysis for saw cutting requirements of concrete pavements. In *Transportation Research Record 2020*: 20-29. TRB, National Research Council, Washington, D.C.

Grasley, Z.C. 2006. *Measuring and Modeling the Time-Dependent Response of Cementitious Materials to Internal Stresses.* Ph.D. Thesis. University of Illinois. Urbana, IL.

Ioannides, A.M. & Khazanovich, L. 1998. Nonlinear temperature effects on multilayered concrete pavements. ASCE Journal of Transportation Engineering 124(2): 128-136.

Rasmussen, R.O. & Rozycki, D.K. 2001. Characterization and modeling of axial slab-support restraint. In *Transportation Research Record* 1778: 26-32. TRB, National Research Council, Washington, D.C.

Roesler, J. R., Bordelon, A., Ioannides, A. M., Beyer, M., and Wang, D. 2008. *Design and Concrete Material Requirements for Ultra-Thin Whitetopping*, Illinois Center for Transportation Series No. 08-016, University of Illinois, Urbana, IL, 181 pp.

Roesler, J. & Wang, D. 2008. An Analytical Approach to Computing Joint Opening in Concrete Pavements. Proceedings of the 6th RILEM International Conference on Cracking in Pavements, June 2008, Chicago, to appear.

Timoshenko, S.P. & Goodier, J.N. (Third Edition) 1970. *Theory of Elasticity*. McGraw-Hill, Inc., page 4.

Westergaard, H.M. 1926. Analysis of stresses in concrete pavements due to variations of temperature. *Proc. Highway Research Board*, Vol. 6: 201-215.

Wimsatt, A.W., McCullough, B.F. & Burns, N.H. 1987. *Methods of analyzing and factors influencing frictional effects of subbases*. Center for Transportation Research, University of Texas at Austin, Research Report 495-2F.

Zhang, J. & Li, V.C. 2001. Influence of supporting base characteristics on shrinkage-induced stresses in concrete pavements. *ASCE Journal of Transportation Engineering* 127(6): 455-462.